ISSN 1063-7729, Astronomy Reports, 2010, Vol. 54, No. 11, pp. 1019–1031. © Pleiades Publishing, Ltd., 2010.
Original Russian Text © B.P. Artamonov, V.V. Bruevich, A.S. Gusev, O.V. Ezhkova, M.A. Ibrahimov, S.P. Ilyasov, S.A. Potanin, Yu.A. Tillaev, Sh.A. Ehgamberdiev, 2010, published in Astronomicheskiĭ Zhurnal, 2010, Vol. 87, No. 11, pp. 1106–1119.

Seeing and Atmospheric Extinction at Mt. Maidanak Observatory from Observations with the 1.5-m AZT-22 Telescope

B. P. Artamonov[1], V. V. Bruevich[1], A. S. Gusev[1], O. V. Ezhkova[1], M. A. Ibrahimov[2], S. P. Ilyasov[2], S. A. Potanin[1], Yu. A. Tillaev[2], and Sh. A. Ehgamberdiev[2]

[1]*Sternberg Astronomical Institute of Moscow University, Universitetskiĭ pr. 13, Moscow, 119992 Russia*

[2]*Ulugh Beg Astronomical Institute, Uzbek Academy of Sciences, Astronomicheskaya Str. 33, Tashkent, 100052 Uzbekistan*

Received May 11, 2010; in final form, June 8, 2010

Abstract—We have determined the realistic seeing of the 1.5-m AZT-22 telescope of the Mt. Maidanak Observatory (Astronomical Institute, Uzbek Academy of Sciences) using more than 20 000 CCD frames with stellar images in the $UBVRI$ bands acquired in 1996–2005: $\epsilon = 1.065''$ in the V band. The characteristic seeing reduced to unit air mass, $\epsilon^V_{med}(M(z) = 1)$, is $0.945''$. We derived color equations for the CCD detectors used with the telescope. Atmospheric-extinction coefficients in different photometric bands were also determined. The mean V-band atmospheric extinction is $0.20^m \pm 0.04^m$. The time needed for the conditions to settle, in the free atmosphere as well as inside the telescope dome, is 2–2.5 hours after the end of astronomical twilight. For nights with $\epsilon^V_{med} < 0.9''$, we find a persistent difference between the seeing found at this telescope and measured simultaneously with a differential image motion monitor, amounting to $\sim 0.1^m$.

DOI: 10.1134/S1063772910110077

1. INTRODUCTION

In the 1960s, various searches were initiated for promising sites for new-generation 3–4-meter telescopes. Sites with large numbers of clear nights and good seeing were found at the western high-altitude plateau of the Andes in Chile, as well as atop volcanic mountains of Hawaii and the Canaries. The Sternberg Astronomical Institute (SAI) of Moscow State University began 9ts first studies of the astronomical conditions at the most promising sites in Middle Asia by the end of the 1960s: at Mt. Sanglok (Tajikistan) and Mt. Maidanak (Uzbekistan). The history of studies at both mountains was described in detail by Shcheglov [1], an enthusiastic pioneer of astronomical climate studies and the establishment of Moscow State University's observatory in Middle Asia.

During the same time, the Ulugh Beg Astronomical Institute (UBAI) of the Uzbek Academy of Sciences arranged studies of the astronomical conditions in various parts of Uzbekistan and, together with the SAI, performed observations at Mt. Maidanak, located in Qashqadaryo province of Uzbekistan, on the slopes of the Baisun range, at an altitude of 2600 m. The closest towns, Kitab and Shahrisabz, are 70–80 km to the north of Mt. Maidanak, and are blocked by the 3000-m-high Tahta range. The light pollution from these towns can be noticed at low altitudes in the north; there is no light pollution to the south and east, down to the horizon; the mountains gradually become lower to the west, where the major settlements are in the plains, far from Mt. Maidanak. One of the principal criteria used to select the telescope site was that the peak be isolated; this criterion was used by Stock [2] to select several peaks in Chile for the European Southern Observatory (ESO). An isolated peak in the 2000–3000-m altitude range should be in the free-atmosphere zone [3]. The surface layer of the Earth quickly cools at night due to its infrared radiation, in turn cooling a thin near-ground air layer that flows downwards along the slopes of the isolated mountain.

In the same period, prospects for acquiring a multi-purpose telescope about 1.5 m in diameter and capable of addressing many observational problems, from wide-field imaging to spectroscopy, were discussed at the SAI. Finally, technical specifications were developed together with the Leningrad Optics and Mechanics Amalgamation (LOMO) on the design of a 1.5-m Ritchey–Chrétien telescope, designated the AZT-22. The design of the dome and tower was simultaneously developed at the Central

Institute for Steel Structures. The AZT-22 telescope was installed at Mt. Maidanak at the end of the 1980s, and made its first light detection in 1991. However, the telescope was not officially completed by the LOMO: the dissolution of the USSR led to the end of the inauguration tests. Currently, the AZT-22 belongs to the Mt. Maidanak Observatory of the UBAI. It has been used for systematic observations since 1995, including as part of cooperative programs of the UBAI and SAI.

2. THE AZT-22 TELESCOPE

2.1. Mount

The AZT-22 telescope (LOMO) has an equatorial fork mount that smaller in size than the English and German mounts. A Ritchey–Chrétien optical system with a relative aperture of 1 : 8 was selected.

The telescope tube was made as a classical Surrier frame. The hour drive is based on a worm gear with a cogwheel diameter of 1.5 m. The worm gear is under a large stress, because it drives both the telescope's hour drive and its rough pointing. A similar worm gear was installed at the declination axis. No mechanical damage was detected in 20 years of use of the telescope, testifying to the high quality of the manufacturing of the worm gears. The telescope is pointed to a target using an analog autosyn system. Two digital "angle–code" sensors are installed on the major worm axes, enabling the possibility of digital telescope pointing in right ascension and declination.

A controller for digital telescope pointing was designed and manufactured in the SAI in 1995, but tests demonstrated that the normal functioning of the digital pointing required preliminary adjustment of all gears, minimizing mechanical play. In 2005, Potanin [4] analyzed errors of the telescope's hour drive during a test of the optical compensator of the wavefront slope. Periodic hour-drive errors result from the rotation of both the main worm and secondary gears, but, in total, result in a mean error of about 0.3″. Using an automated guide based on the above device, which works at high frequencies, makes it possible to compensate for such small hour-angle deviations, reducing them to values below the telescope's optical aberrations. Differential bending of the telescope fork mount results in systematic image displacements in the focal plane, especially at low elevations, limiting exposure times for program objects with CCD cameras to three to five minutes. Astronomers from Kharkov National University developed an automated platform with an automated guide used to mount a CCD camera and installed it in 2007, making possible a considerable increase of the exposure time.

2.2. Optical Systems

The design of the optical system of the telescope was presented by the LOMO opticians [5], and independently by Artamonov and Tertitsky [6]. A two-mirror quasi-Ritchey–Chrétien system with a relative aperture of 1 : 8 was selected as the principal optical system of the telescope, with a two-lens quartz corrector designed to provide a 1.5-degree field of view. A five-lens quartz focal reducer with a relative aperture of 1 : 3 for a field of 1° was designed and manufactured. A two-lens quartz corrector with a different secondary mirror was designed for the 1 : 17 optical system for a field size of 100 mm. A four-mirror Coudé-focus system with its own secondary mirror was also designed. Note that this set of optical systems was due to the requirements for a universal university telescope. Currently, the 1 : 8 system without a corrector, and sometimes the 1 : 17 system with a corrector are used for observations. The existing technical parameters of CCD cameras do not permit the use of the wide-field corrector in the 1 : 8 system, due to the small distance between its last lens and the focal plane. The use of CCD cameras with large chips (4×4 K) in the 1 : 8 system requires the design and construction of a new corrector for a field size of about 20′. S.A. Potanin designed a two-mirror quartz corrector for the 1 : 8 system of the telescope, with aberration errors of about 0.2″ over the whole field, over a wide wavelength range (3500–9500 Å), which has a large distance between the last corrector lens and the focal plane, enabling the installation of a filter unit and large CCD camera.

The manufactured optical systems of the telescope were tested at the LOMO workshop using an unequal-length interferometer, one of whose arms was the optical system of the AZT-22 telescope and whose other arm was a reference spherical mirror. Specially designed correctors were applied to correct for path-length differences between the telescope's optical system and the reference sphere exceeding one wavelength. Measurements of the resulting interference patterns were used to derive the telescope optical-system parameters and compare them with calculations. The results of the LOMO workshop tests of all optical systems of the telescope are collected in [7], and demonstrate the good quality of the optics made at the LOMO. As an example, Fig. 1a displays the energy distributions within circlular apertures (in arcseconds) for the 1 : 8 system without a corrector. The calculated light energy density differs from the workshop measurements by about 2–3%, clearly testifying that the optics of the AZT-22 telescope created at the LOMO nearly reaches the diffraction limit. Similar results were obtained for other optical systems of the telescope.

A large problem in exploiting the high-quality telescope optics is fine tuning of the optical system at the telescope site, as well as the correct functioning of the main mirror's off-loading system. To check the optical tuning and functioning of the off-loading, Potanin [8] tested the optical quality of the telescope with a wavefront sensor in 2008; the method used to study the quality of the telescope optics is described in [8]. For comparison with the calculations and workshop tests of the telescope's 1 : 8 optical system with no corrector, Fig. 1b shows the energy densities within circular apertures with various sizes measured at the Mt. Maidanak Observatory. The differences between the calculated and measured energy densities for the 1 : 8 optical system can reach 10% for some apertures. To improve the optical characteristics of the telescope, i.e., to approach those found during the workshop tests, finer tuning of the primary and secondary mirrors and adjustment of the main-mirror off-loading are needed. Nevertheless, the optics of the AZT-22 telescope of the Mt. Maidanak Observatory are almost diffraction quality, and this is clearly the best telescope produced by LOMO, particularly also taking into account the high quality of the telescope mechanics.

Fine mirror adjustment of the AZT-22 telescope was begun by O.I. Bugaenko in 1991–1992. He developed techniques and special devices for tuning the primary mirror by combining the optical axis and the mechanical rotation axis of the bearing whose flange is used to install the detecting equipment (e.g., a CCD camera). The secondary mirrors were tuned by combining their optical axes with the axis of the primary mirror. In 2008, a team of astronomers from the Kharkov National University headed by V.N. Dudinov repeated the mirror tuning of the AZT-22 telescope using an improvement of the technique proposed by O.I. Bugaenko. S.A. Potatin took part in this work.

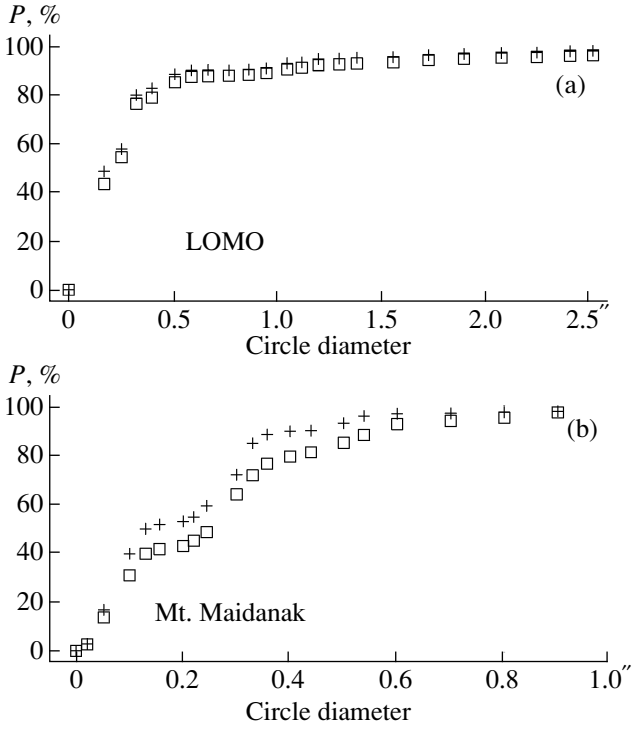

Fig. 1. Energy densities within circular apertures, P, for the 1 : 8 optical system of the AZT-22 telescope without a corrector. The calculated energy densities (crosses) and the energy densities measured (a) in tests at the LOMO workshop (squares) and (b) under field conditions are shown.

3. THE ASTRONOMICAL CLIMATE OF Mt. MAIDANAK AND INSIDE THE AZT-24 DOME

In 1975, the SAI performed measurements of the astronomical climate at the western and eastern peaks of Mt. Maidanak, located at a distance of about 10 km. The two peaks are compared in [9]. Both peaks were found to have similar parameters, but the western peak provides better conditions for construction works, leading it to be selected for Moscow State University's observatory. Visual estimates of the seeing, ϵ, were obtained for both peaks with a two-beam instrument via systematic observations of Polaris in the Summer and Autumn of 1975; on average, these indicated $\epsilon = 0.6''$. The central peak of Mt. Maidanak is 4 km to the east of the western peak; the AZT-24 telescope, as well as the AZT-14 and Zeiss-600 telescopes of the UBAI, are installed at the central peak. In this paper, the term "Mt. Maidanak Observatory" refers to the observatory on the western peak of Mt. Maidanak. Studies of the astronomical climate conditions at the central peak were organized and performed in the 1960s and 1970s by astronomers from the UBAI and SAI [1].

The results of extensive studies of the observing conditions at Mt. Maidanak performed in the 1960s and 1970s were confirmed in 1996–1999 with a series of observations of the astronomical climate using modern techniques [10, 11]. The Differential Image Motion Monitor (DIMM) was installed near the 1.5-m AZT-22 telescope of the Mt. Maidanak Observatory, five meters above the ground. The four-year observations revealed a mean seeing of $0.69''$. Later studies of the atmosphere at Mt. Maidanak with the MASS instrument [12] detected a free-atmosphere seeing of $0.47''$ at heights of 0.5 km and more above the level of Mt. Maidanak.

Obtaining high-angular-resolution images requires the design of a telescope dome that does not introduce any considerable seeing aberrations.

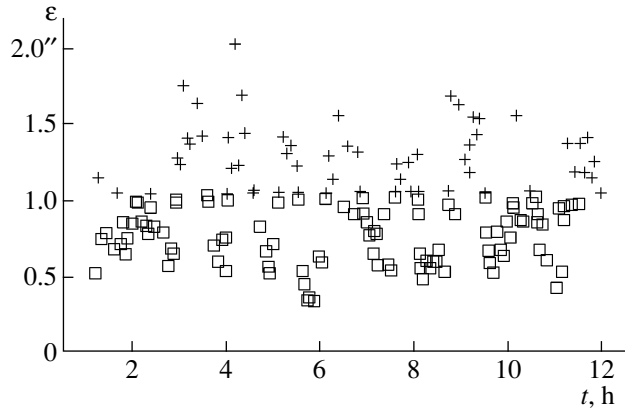

Fig. 2. Seeing ϵ under the dome of the AZT-24 telescope. Crosses and squares show the seeing with the ventilation off and on. The time interval between switching the ventilation on and off was about 30 minutes.

Such a project for the AZT-22 dome was developed by Novikov and Ovchinnikov [13] in cooperation with engineers of the Central Institute for Steel Structures. The telescope dome is 12 m in diameter, and consists of two shells separated by 80-cm, making it possible to stabilize the temperature of the space inside the dome during day-time heating, and to retain the night temperatures. The outer shell is assembled of hexagonal panels (a sandwich of aluminum and foam plastic). The inner shell sides are coated with thick polyurethane-foam layers. This thermal insulation prevents dome heating during the day, making it possible to maintain night-time temperatures under the dome. A ventilation system installed in the telescope tower sucks free-atmosphere air through the dome opening, making it possible to suppress turbulent flows under the dome (the telescope is cooled with the colder ambient air) and forming a quasi-laminar air flow during night-time observations. Some functioning results of the ventilation system at the Mt. Maidanak AZT-22 telescope are discussed in [14].

Table 1. Numbers of CCD frames for years and filters

Year	U	B	V	R	I	Total
1996	–	48	151	166	86	451
1997	–	674	945	1033	513	3165
1998	–	265	664	851	363	2143
1999	–	1266	300	1116	251	2933
2000	591	397	374	527	379	2268
2001	15	29	80	174	76	374
2002	629	513	807	899	632	3480
2003	248	247	606	1979	353	3433
2004	109	104	146	396	163	918
2005	279	275	296	1274	321	2445
Total	1871	3818	4369	8415	3137	21 610

The influence of the space under the dome was analyzed and described in [15]. These experiments were carried out using the AZT-24 telescope (with a main-mirror diameter of 1.1 m) installed on the central peak of Mt. Maidanak, 4 km from the AZT-22. The tower design of the AZT-24 telescope is similar to that of the AZT-22, but there are differences in the dome design. A DIMM was installed under the dome of the AZT-24, to the south of the telescope foundation. The seeing was measured with the DIMM on September 26–27, 1997, with the control equipment of the AZT-24 turned on. There are three strong ventilation systems under the dome, which create a flow of air from outside through the open dome slit and evacuate air via a windpipe to a gorge at a large distance from the tower. There are two heating sources under the dome: residual heating from day-time heating of the tower and telescope, and heating from working equipment. The DIMM measures the motion of a stellar image in the CCD frame and estimates the seeing in arcseconds. The results of these measurements are shown in Fig. 2, where different symbols show the measured seeing in arcseconds during periods when the strong ventilation system was on and off. Each of these periods had a duration of 30 minutes, making it possible to follow several cycles during a night. The mean seeing with the ventilation off and was 1.3″ and 0.7″. We also studied the time for the seeing to stabilize (for the temperature of the ambient air and the space under the dome to equalize). With the ventilation off, this is about 3 hours, while it is about 1.5–2 hours with the ventilation on; however, in the latter case, this time is also related to the stabilization of the outside atmosphere, which depends on the time for the ground and atmosphere to cool after day-time heating (also about 2 hours, see Fig. 7a below).

4. SEEING AT THE AZT-22 TELESCOPE

4.1. Observations and Processing

Some seeing estimates for the AZT-22 telescope can be found in [16–18] and in later papers on gravitational-lens monitoring.

To estimate the seeing based on a large sample of CCD observations obtained at the 1.5-m telescope, we used CCD images (21 610 frames) of various astronomical objects in the U, B, V, R, and I filters available at the SAI. These observations were performed in 1996–2005 with a TI 800 × 800 CCD camera (1996–1999) and an SITe 2000 × 800 CCD

camera (2000–2005). The distributions of these observations in time (years) and over filters is presented in Table 1. The seeing estimates for the 1.5-m can be compared to the 1996–1999 DIMM data obtained when this instrument was mounted near the AZT-22 tower.

We estimated the seeing using the sizes of stars in the CCD frames, taking a star's visible size to be its FWHM profile diameter. The results were then translated into seconds of arc. For most of the images we used, the scale is 0.2667″ per pixel (short-focus observations, 1 : 8). Some observations were obtained in the long-focus mode, 1 : 17 (with a scale of 0.1333″ per pixel). The TI 800 × 800 CCD used in our observations has two operation modes: 800 × 800 and 400 × 400. The scale for the latter mode is 0.5333″ per pixel (short-focus observations, 1 : 8) or 0.2667″ per pixel (long-focus observations, 1 : 17).

Typical exposure times of our observations were 5–300 s.

4.2. Dependence of the CCD Seeing on Exposure Time and Air Mass

Our data analysis reveals that, when the seeing is very good ($\epsilon < 0.8''$) and the exposure time is below 3 minutes, there is a weak dependence between the image size and the exposure time:

$$\epsilon(t) \approx (0.0003-0.0004)t + \text{const}, \qquad (1)$$

where t is the exposure time in seconds. This corresponds to the above-mentioned inaccuracy of the telescope drive in hour angle, which shifts objects by $0.1''-0.2''$ in two to three minutes. To remove the $\epsilon(t)$ dependence, we measured the sizes of stellar images along the declination axis, δ, which are independent of the exposure time.

As an example, Fig. 3 displays the seeing ϵ as a function of exposure time for eight nights with median seeing, $\epsilon^V_{med} \leq 0.85''$ (September 5–6, 7–8, 9–10, 10–11, 2002 and November 23–24, 24–25, 25–26, 27–28, 2003), using only frames taken no earlier than three hours after sunset (a total of 148 CCD frames in the V and R bands), and excluding observations obtained during the relaxation to the stationary temperature regime under the dome.

The stellar-image sizes also depend on the air mass. Figure 4 shows the dependence of the seeing ϵ on the air mass $M(z)$ for the same set of measurements as in Fig. 3. For seeing $\epsilon < 0.9''$ and air masses $M(z) \equiv \sec z < 1.6$, there is a known relation for the seeing: $\epsilon(z)$ [19]:

$$\epsilon(z) = \epsilon(0)M(z)^{3/5}. \qquad (2)$$

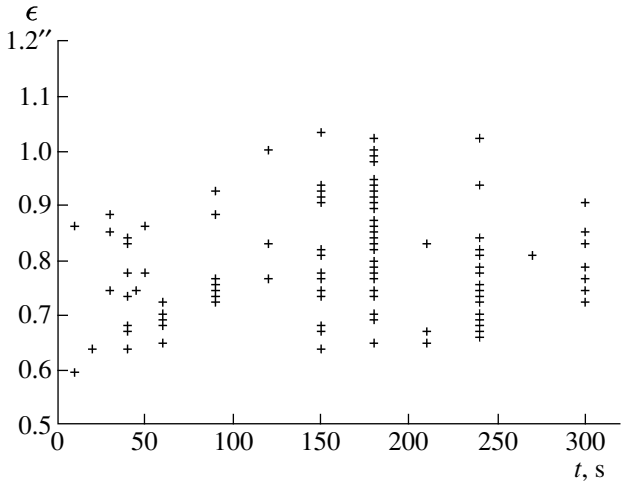

Fig. 3. Seeing ϵ from the V and R CCD images as a function of exposure time t for eight nights with good ϵ^V_{med}.

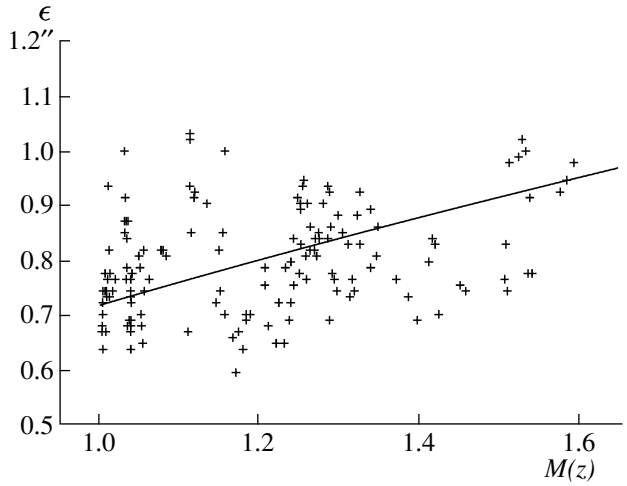

Fig. 4. Seeing ϵ from V and R CCD images as a function of air mass $M(z)$ for eight nights with good ϵ^V_{med}. The solid curve is the $\epsilon(z) \sim M(z)^{3/5}$ relation.

For the data shown in Fig. 4, $\epsilon(0) = 0.72''$. We did not reduce the ϵ values to the air mass $M(z) = 1$, because some 80% of the images have sizes in excess of 0.9″ (see below). They show no obvious relation between ϵ and $M(z)$. Since most of the observations were performed at zenith distances $z < 40°$, corresponding to air masses $M(z) < 1.3$, the sizes of stellar images reduced to unit air mass will be below the observed values by no more than 10–15%.

Below, when comparing the seeing measured at the telescope to the DIMM results, we reduce our data to unit air mass using the procedure described in [19].

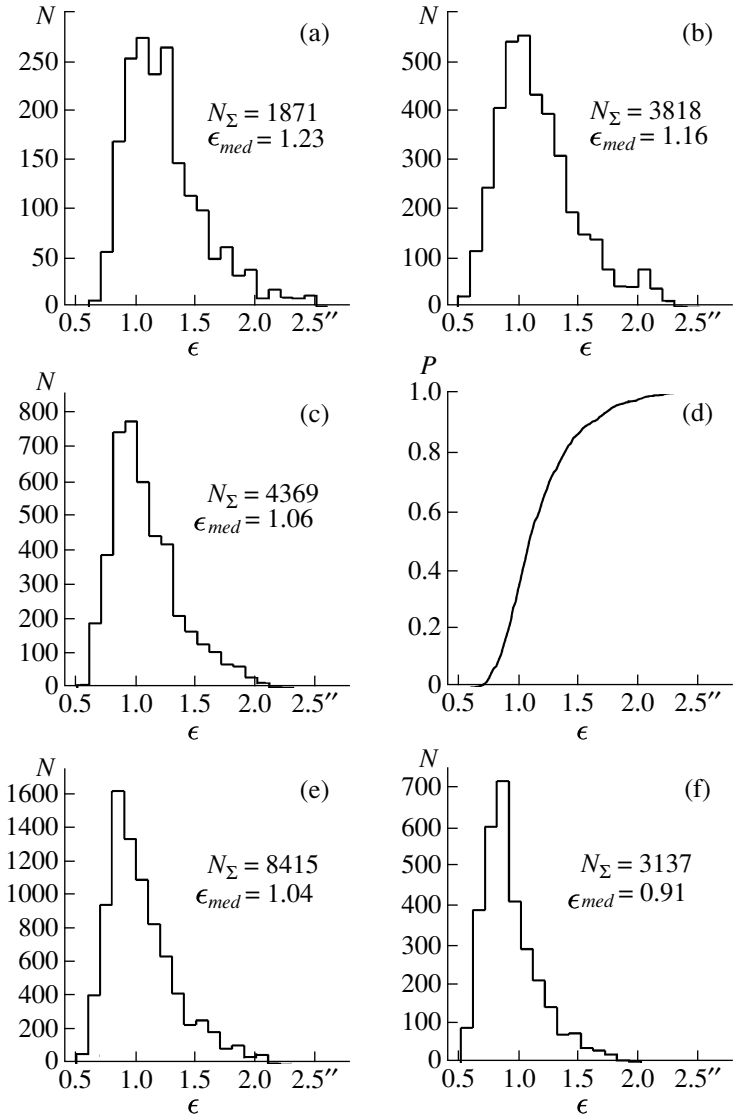

Fig. 5. Distributions of the seeing ϵ measured in the (a) U, (b) B, (c) V, (e) R, and (f) I bands and (d) the integrated seeing distribution in the V band. The total number of frames N_Σ and the median seeing ϵ_{med} are indicated for each band.

4.3. Seeing from CCD Images in Various Filters

Figure 5 presents histograms of the seeing measured in the U, B, V, R, and I bands, as well as the integrated seeing in the V band. The median seeing, ϵ_{med}, ranges from $1.23''$ in U to $0.91''$ in I. The seeing in V varies from $0.5''$ to $2.4''$, with $\epsilon^V_{med} = 1.065''$. The number of images with $\epsilon^V \leq 0.7''$ does not exceed 2%, and the number with $\epsilon^V \leq 0.8''$ does not exceed 8% (Fig. 5d). No photometric observations were carried out with the telescope if $\epsilon > 2.3''-2.7''$. Figure 5 shows that taking into account the dependence of ϵ on exposure time t and air mass $M(z)$ would not change the resulting distribution of ϵ or the values of ϵ_{med}.

The derived median seeing values in the various photometric bands are in good agreement with the following relation between ϵ and λ:

$$\epsilon(\lambda) = (10.52 \pm 0.03)\lambda^{-1/5} + \text{const}, \qquad (3)$$

where λ is the wavelength (in Å) for the maximum transparency of the corresponding filter.

Using the median values $M(z)_{med} = 1.22$ and $\epsilon^V_{med} = 1.065''$ for the AZT-22 frames, we estimated the characteristic seeing reduced to unit air mass, $\epsilon^V_{med}(M(z) = 1)$. According to (2), $\epsilon^V_{med}(M(z) = 1) = 0.945''$. Since, strictly speaking, (2) is valid only for the free atmosphere, our estimate of $\epsilon^V_{med}(M(z) = 1)$ should be treated cautiously.

Note that the minimum sizes of the stellar images measured for the AZT-22 telescope are a factor of

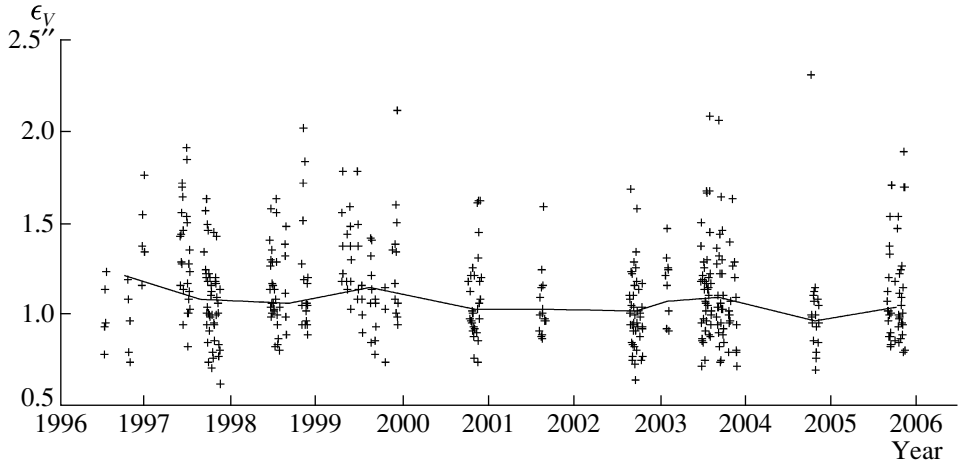

Fig. 6. Nightly (crosses) and yearly (broken line) averages of the V-band seeing ϵ.

three to ten larger than the theoretical diffraction radius (for the $I-U$ bands) .

4.4. CCD Seeing over Years and Months

Figure 6 displays the V-band seeing for each observing night (nightly median ϵ_V values are plotted). In total, we reduced data for 378 nights between July 1996 and November 2005.

The scatter of the nightly mean ϵ_V values is fairly large: from 0.6″ to 2.3″, but the seeing is 0.8″–1.4″ on most nights. During the entire observation period, ϵ_V was better than 0.7″ on only two nights (0.5%) and better than 0.8″ on 31 nights (7%). We found $\epsilon_V >$ 1.6″ for 31 nights (7%), but few CCD frames were taken on such nights, since most observing programs using this telescope require better seeing.

Generally, the distribution of the nightly averaged seeing repeats the distribution for the individual CCD frames (Figs. 5c, 5d), both as a whole and for individual long series of data.

To estimate long-term seeing trends, we calculated the median ϵ_V values for each observation year (year 2003 was subdivided into two, corresponding to Winter and Summer–Autumn). These results are also presented in Fig. 6.

Excluding the data for 1996 (a year with poor statistics, with only 15 observation nights), we find that the seeing did not change during the studied period, on average. The range of ϵ_V was 0.97″ (2005)–1.15″ (1999).

Ehgamberdiev et al. [11] analyzed the seeing at the Mt. Maidanak Observatory for different months. Our analogous analysis for the CCD seeing at the AZT-22 telescope (Table 2) generally reproduces the results of [11]: the best seeing is achieved in Autumn (with the median $\epsilon_V = 1.01''$ for October observations); while the worst seeing is obtained in the Winter–Spring (with ϵ_V reaching 1.44″ in April). February is an exception, with our observations indicating relatively good seeing, $\epsilon_V = 1.08''$ (the worst month according to [11]). The discrepancy between our results and those of [11] concerning the seeing in February is probably due to insufficient statistics of the available CCD observations (only seven nights

Table 2. Distribution of CCD seeing ϵ over months

Month	Number of observation years	Number of observation nights	Total number of frames	ϵ^V_{med}
January	1	2	59	1.29″
February	1	7	459	1.08
March	0	0	0	–
April	1	5	213	1.44
May	2	10	399	1.32
June	4	38	1424	1.34
July	5	63	1838	1.08
August	6	44	1366	1.10
September	6	93	5542	1.06
October	9	93	5186	1.01
November	7	68	4024	1.04
December	3	17	1100	1.29
Total	10	440	21 610	1.06

in 2003). A detailed comparison of our data and the results of [11] will be presented below.

4.5. Time for Relaxation to Stationary Conditions in the Free Atmosphere and Under the AZT-22 Dome

When planning observations, it is important to know the time needed for relaxation to the stationary parameters of the night atmosphere (most importantly, temperature), since the seeing is directly dependent on the atmospheric stability at the observing site. Estimates of the relaxation to stable observing conditions under the AZT-22 dome can be found in [14].

To estimate the time for relaxation to stationary atmospheric conditions under the AZT-22 dome with the ventilation on, we analyzed the variations of the CCD V and R seeing during the course of a night for eight nights with $\epsilon^V_{med} \leq 0.85''$ (September 5–6, 7–8, 9–10, 10–11, 2002 and November 23–24, 24–25, 25–26, 27–28, 2003; a total of 172 CCD frames). Note that, in this case, we used the ϵ values reduced to unit air mass in accordance with (2). The results, presented in Fig. 7b, show that the time scale for relaxation to stationary conditions under the dome is 2–2.5 hours after the end of astronomical twilight. For comparison, Fig. 7a shows the seeing measured on the same nights with the DIMM [11] mounted near the AZT-22 tower.

Simultaneous seeing estimates with the DIMM and at the AZT-22 can be used to estimate the influence of the space under the telescope dome, which is experiencing the thermal influence of the working telescope systems and mounted equipment, as well as to take into account the slow cooling of the tower and dome parts after heating during the day. Figure 7b shows fourth-order polynomial fits for the DIMM and AZT-22 that average the seeing during a night. The seeing in the free atmosphere differs from that under the dome by about $0.1''$ when the ventilation is on. The experiment on reducing the turbulence under the dome of the AZT-24 telescope described above has demonstrated that a powerful ventilation system is able to create a laminar flow and to improve the seeing to within 15 minutes. The AZT-22 ventilation system is probably not strong enough to provide an appreciable improvement in the seeing. It appears that the relaxation of the thermal conditions under the AZT-22 dome takes approximately the same time as in the free atmosphere. The difference between the DIMM and AZT-22 estimates remains constant, and this remains unexplained for the moment. Note that a similar difference was observed by Chinese astronomers during simultaneous seeing estimates with a one-meter telescope at the Yunnan Observatory and a DIMM installed near its tower ($1.17''$ and $0.84''$, respectively) [20]. The limits on the seeing measured for the AZT-22 telescope with its nearly diffraction-quality optics are mainly related to conditions in the space under the dome, which could be changed if a new, higher-power ventilation system is introduced. Achieving seeing comparable to the diffraction limit for the telescope optics will require the introduction of an adaptive-optical system that compensates for turbulence in the free atmosphere. As was demonstrated in [12], such a system would be effective for the observing conditions at Mt. Maidanak.

In our opinion, our comparison of the DIMM and AZT-22 measurements is only preliminary. A deeper analysis of the influence of the space under the dome on the seeing requires a specially designed experiment with a DIMM installed on the AZT-22 telescope tube for simultaneous observations on nights with various conditions in the free atmosphere, as well as with the ventilation system on and off, and with temperature fluctuations measured at different positions of the tower. Such experiments will help to improve the ventilation system in the AZT-22 tower.

5. ATMOSPHERIC EXTINCTION AT MT. MAIDANAK OBSERVATORY AND THE INSTRUMENTAL PHOTOMETRIC SYSTEM OF THE AZT-22 TELESCOPE

5.1. Color Equations for the Instrumental Photometric Systems of the AZT-22 Telescope

A detailed analysis of the atmospheric extinction and the color-equation coefficients was independently performed by Korean astronomers using observations obtained in 2003–2007 [21] using an SITe 2000×800 (up to 2005) and Fairchild 4000×4000 (beginning in 2006) CCD. We compare our results to the conclusions of [21] below.

The color equations needed for accurate photometric studies were earlier derived and implemented for the telescope + TI 800×800 CCD system [17, 18], without taking into account their dependence on the atmospheric extinction. Equations transforming the data from the telescope + SIT 2000×800 CCD instrumental system to the standard Johnson–Cousins $UBVRI$ photometric system were obtained and applied in [22, 23]. However, the color-equation coefficients and data on the atmospheric extinction we derived remained unpublished.

To derive the color equations for the telescope + SITe 2000×800 CCD system taking into account atmospheric extinction, we used observations of the standard stars in the Landolt [24] fields RU 149, PG 1047+003, PG 2336+004, SA 95, and SA 98, as well as standard stars in the open cluster NGC 7790

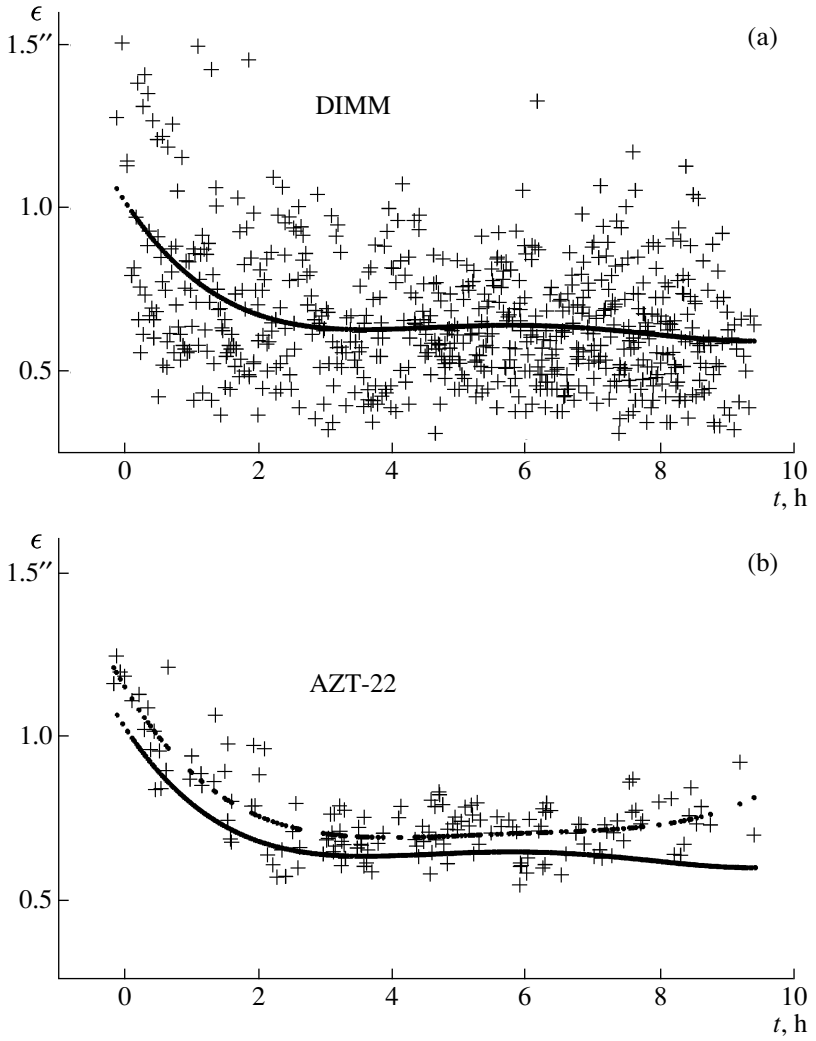

Fig. 7. Comparison of the seeing during the course of a night measured (a) with the DIMM and (b) at the AZT-22. DIMM data for eight nights with good ϵ values averaged with a fourth-power polynomial are shown together with the V and R AZT-22 data (ϵ_V and ϵ_R, reduced to unit air mass) for the same nights, averaged with a fourth-power polynomial. The time 0 hours correspond to the end of astronomical twilight.

[25]. These observations were performed on November 8–9, 9–10, 26–27, and 27–28, 2003 with the U, B, V, R, and I filters, for air masses $M(z) = 1.1$–1.9. $UBVRI$ photometry was obtained for 88 stars; the fluxes for 65 stars were measured at different $M(z)$ values.

The color equations for the telescope + TI 800 × 800 CCD system taking into account atmospheric extinction were obtained from $BVRI$ photometry of Landolt standard stars [24] (the fields PG 1657+078 and SA 110; a total of eight stars). The observations were performed on July 6–7 and 7–8, 1997 for air masses $M(z) = 1.4$–1.7. The results of these photometric measurements of standard stars obtained in 1997 were earlier used in [17, 18].

To transform the data from the instrumental to the standard system, we calculated coefficients of the color equations of the form

$$\begin{aligned} F_1 = {} & C_{f_1}^{f_1} f_1(t_{f_1}, M_{f_1}(z)) \\ & + C_{f_1}^{f_1 f_2}(f_1(t_{f_1}, M_{f_1}(z)) - f_2(t_{f_1}, M_{f_1}(z))) \\ & + C_{f_1}^{M(z)} M_{f_1}(z) + C_{f_1}^{f_1 f_2 M(z)}(f_1(t_{f_1}, M_{f_1}(z)) \\ & - f_2(t_{f_1}, M_{f_1}(z)))M_{f_1}(z) + C_{f_1}^{t} + 2.5 \log t_{f_1}, \end{aligned} \tag{4}$$

where F_1 is the magnitude in the F_1 band of the standard photometric system; f_1, f_2 are the magnitudes in the f_1, f_2 bands of the instrumental photometric system; t_{f_1} is the exposure time (in seconds) for the frame taken in the f_1 filter; $M_{f_1}(z)$ is the air mass for the frame taken in the f_1 filter; $C_{f_1}^{f_1}$, $C_{f_1}^{f_1 f_2}$, $C_{f_1}^{M(z)}$, $C_{f_1}^{f_1 f_2 M(z)}$, $C_{f_1}^{t}$ are the equation's coefficients; and

Table 3. Color-equation coefficients and their uncertainties for the telescope + SITe 2000 × 800 CCD and telescope + TI 800 × 800 CCD systems

f_1	$C_{f_1}^{f_1 f_2}$		$C_{f_1}^{M(z)}$
	2000 × 800 CCD detector	800 × 800 CCD detector	
u	-0.139 ± 0.040	–	-0.582 ± 0.143
b	0.111 ± 0.016	0.325 ± 0.014	-0.339 ± 0.051
v	-0.020 ± 0.013	0.074 ± 0.009	-0.202 ± 0.036
r	0.012 ± 0.028	0.018 ± 0.013	-0.110 ± 0.053
i	0.024 ± 0.018	0.089 ± 0.007	-0.061 ± 0.048

$f = -2.5 \log l$ are magnitudes (l being the measured light flux).

We found when calculating the color-equation coefficients that the coefficients of the form $C_{f_1}^{f_1 f_2 M(z)}$ were small compared to the uncertainties in the other coefficients, making it possible to neglect them without deteriorating the accuracy.

For observations in the linear dynamic range of a CCD chip, the $C_{f_1}^{f_1}$ coefficients are usually assumed to be unity. We undertook an additional study of the $C_{f_1}^{f_1}$ values and confirm that $C_{f_1}^{f_1} = 1$ within the errors.

Thus, the color equations are reduced to the form

$$F_1 = f_1 + C_{f_1}^{f_1 f_2}(f_1 - f_2(t_{f_1}, M_{f_1}(z))) + C_{f_1}^{M(z)} M(z) + C_{f_1}^{t} + 2.5 \log t. \quad (5)$$

The $f_2(t_{f_1}, M_{f_1}(z))$ relation means that, when using (5), the fluxes in the f_1 and f_2 filters must be normalized to the same exposure time and unit air mass.

Thus, we used the following color equations to transform data from the instrumental $ubvri$ system to the standard $UBVRI$ photometric system:

$$U = u + C_u^{ub}(u - b) + C_u^{M(z)} M(z) + C_u^{t} + 2.5 \log t, \quad (6)$$

$$B = b + C_b^{bv}(b - v) + C_b^{M(z)} M(z) + C_b^{t} + 2.5 \log t, \quad (7)$$

$$V = v + C_v^{bv}(b - v) + C_v^{M(z)} M(z) + C_v^{t} + 2.5 \log t, \quad (8)$$

$$R = r + C_r^{vr}(v - r) + C_r^{M(z)} M(z) + C_r^{t} + 2.5 \log t, \quad (9)$$

$$I = i + C_i^{vi}(v - i) + C_i^{M(z)} M(z) + C_i^{t} + 2.5 \log t. \quad (10)$$

For observations with the TI 800 × 800 CCD, which is insensitive in the U band, the set of Eqs. (7)–(10) should be used.

The derived coefficients $C_{f_1}^{f_1 f_2}$ and $C_{f_1}^{M(z)}$ and their uncertainties are collected in Table 3 (the second column is for the telescope + SITe 2000 × 800 CCD system and the third for the telescope + TI 800 × 800 CCD system).

The $C_{f_1}^{M(z)}$ coefficients represent the atmospheric extinctions derived from our observations ($K(f_1) = -C_{f_1}^{M(z)}$). The problem of atmospheric extinction will be considered in more detail in the next section.

We do not present any numerical data for the C^t terms ("zero points"), since, strictly speaking, these are valid only for particular dates of observations (for November 2003 and July 1997, respectively). The C^t coefficients mainly depend on dust contamination of the telescope mirrors and filters and on the atmospheric conditions, and change with time.

The presented coefficient C_u^{ub} and Eq. (6) are fairly preliminary because of the large uncertainty due to the low number of standard-star observations at different air masses during a night. Both instrumental systems are close to the standard photometric system for the V and R bands.

The color equations derived independently by Ibrahimov [26] (from observations in August 2001) and Zheleznyak [27] (from observations in October 2000) have the same coefficients within the errors. The color-equation coefficients derived in [21] for the telescope + SITe 2000 × 800 CCD differ slightly from our values ($C_b = 0.053 \pm 0.003$, $C_v = -0.043 \pm 0.002$, $C_i = 0.054 \pm 0.002$; C_r was not derived). The C_u coefficient derived in [21] is considerably different from our own estimate (Table 3). Note, however, that Lim et al. [21] derived their color equations based on the SAAO system, which differs strongly from the U-band data of Landolt [24].

Given that the color equations [21] are based ona large amount of statistical material, we can recommend their use for the telescope + SITe 2000 × 800 CCD system in the B, V, I filters and for the telescope + Fairchild 4000 × 4000 CCD in the B,V, R, and I filters. It is possible to apply the C_u coefficient derived in [21], bearing in mind the difference between the SAAO and Landolt standards.

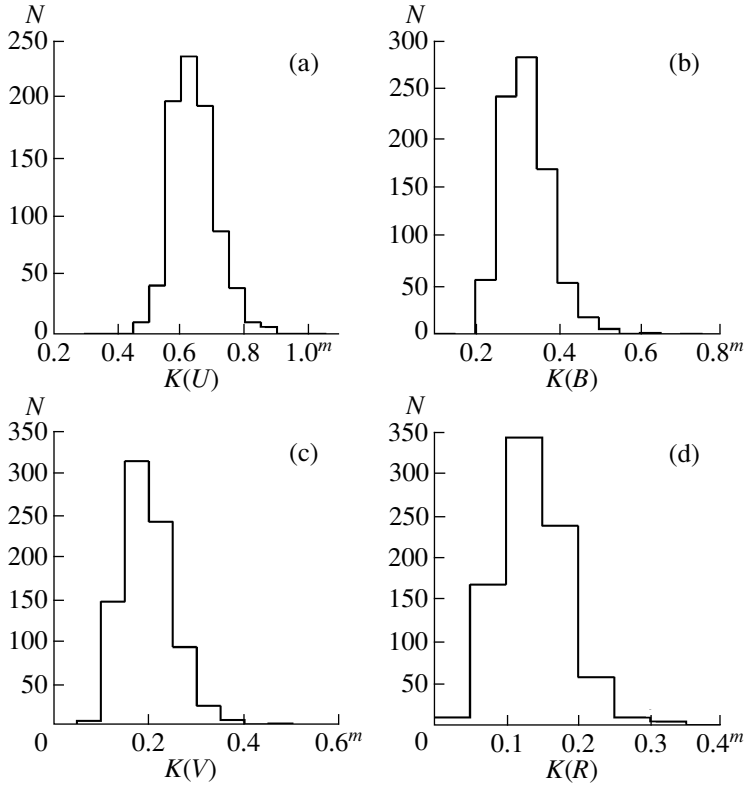

Fig. 8. Distributions of nightly-mean atmospheric extinction at the central peak of Mt. Maidanak in 1991–2002 for the (a) U, (b) B, (c) V, and (d) R_J bands.

5.2. Atmospheric Extinction at Mt. Maidanak Observatory

We used the results of our absolute $UBVRI$ photometry of standard stars to estimate the atmospheric extinction in the corresponding bands (the $C^{M(z)}$ coefficients in (6)–(10); Table 3). The extinction we found for the V band, $K(V) = 0.20^m \pm 0.04^m$, is in good agreement with earlier estimates: 0.21^m [28, 29] (studies of 1976–1998), $0.15^m \pm 0.02^m$ [26], 0.18^m [27], and $0.18^m \pm 0.05^m$ [21]. The large uncertainty in our estimate (20%) is due to large variations of the atmospheric extinction. Special studies by astronomers from Lithuania [29], Uzbekistan [30], and Korea [21] have demonstrated that the atmospheric extinction at Mt. Maidanak Observatory varies within 0.08^m–0.45^m in the V band [29], and nightly variations can reach 0.2^m (recorded on August 15–16, 1977) [28]. The atmospheric extinction depends on the season: it is minimum in January–March (0.11^m–0.14^m) and maximum in July–August (0.20^m–0.22^m) [21, 31]. A strong correlation between atmospheric extinction and relative humidity was detected [30]. All these findings reflect the known dependence of the atmospheric extinction on the amount of dust in the atmosphere.

The extinction we derived for the U–I bands is also in good agreement with data from earlier studies [21, 26, 29–31], and the ratios for the different bands are close to model relations calculated from observations at the European Southern Observatory in Chile [32]. In particular, the mean extinction at the Mt. Maidanak Observatory (central peak) from observations of 1991–2002 (833 nights) is $0.64^m \pm 0.07^m$ (median 0.63^m) in the U band, $0.33^m \pm 0.06^m$ (median 0.32^m) in B, $0.20^m \pm 0.05^m$ (median 0.19^m) in V, and $0.14^m \pm 0.05^m$ (median 0.13^m) in R_J [31]. According to [21] (25 observing nights in 2003–2007), the mean extinction at the western peak of Mt. Maidanak (the site of the AZT-22 telescope) is $0.49^m \pm 0.07^m$ in U, $0.29^m \pm 0.05^m$ in B, $0.18^m \pm 0.05^m$ in V, $0.12^m \pm 0.04^m$ in R, and $0.08^m \pm 0.06^m$ in the I band. The extinction was higher than the mean value by approximately 0.05^m in all bands during the Spring–Summer season and smaller by 0.05^m during the Autumn–Winter season [21]. Figure 8 shows previously unpublished distributions of the atmospheric extinction coefficients in the $UBVR_J$ bands from observations in 1991–2002 [31].

During the Summer period, the atmospheric extinction at the Mt. Maidanak Observatory is a factor

of 1.5–2 higher than at the best observatories in Chile, Hawaii, or the Canaries [33].

6. CONCLUSIONS

1. After the testing of its optics in the LOMO workshop and at the observatory site, the Mt. Maidanak 1.5-m AZT-22 telescope has displayed an almost diffraction-limited quality. Given its excellent mechanical properties, it can be considered one of the best LOMO telescopes.

2. We have estimated the seeing of the 1.5-m AZT-22 telescope using CCD imaging (21 610 frames) in the U, B, V, R, and I filters performed in 1996–2005. The median seeing at the telescope site is $\epsilon^V_{med} = 1.065''$. The number of frames with $\epsilon^V < 0.8''$ is no greater than 8% (7% of all nights had $\epsilon^V_{med} < 0.8''$). We estimate the characteristic seeing reduced to unit air mass, $\epsilon^V_{med}(M(z) = 1)$, as $0.945''$.

3. Our comparison of the seeing measured simultaneously at the telescope and with a DIMM installed close to the AZT-22 tower enabled us to estimate the influence of the space under the dome on the seeing. After stabilization of the temperature conditions in the free atmosphere and under the AZT-22 dome with the ventilation turned on, the nights with $\epsilon^V_{med} < 0.9''$ demonstrate a constant difference of about $0.1''$ between the DIMM and AZT-22 seeing estimates, which remains unexplained.

4. The best seeing is in Autumn ($\epsilon_V = 1.01''$ in October), while the worst is during the first half of each year ($\epsilon_V = 1.44''$ in April). The yearly-averaged seeing generally did not vary in 1996–2005.

5. The seeing does not depend on the exposure time and shows a weak dependence on the air mass (for $M(z) \leq 1.6$) in cases when $\epsilon_V > 0.9''$.

6. The time scale for the relaxation to stationary atmospheric conditions at the Mt. Maidanak Observatory is about 2–2.5 hours after the end of astronomical twilight.

7. The mean V-band atmospheric extinction is $K(V) = 0.20^m \pm 0.04^m$.

Finally, we note that our results are of importance for planning observations, performing new experiments to study turbulence under the dome, and adjusting the telescope's optical systems and mechanical units in order to acquire images with high angular resolution.

ACKNOWLEDGMENTS

The authors wish to thank V.G. Kornilov (SAI) for helpful discussions of this paper. This work was supported by the Russian Foundation for Basic Research (project nos. 08-02-01323 and 09-02-00244).

REFERENCES

1. P. V. Shcheglov, *Problems of Optical Astronomy* (Nauka, Moscow, 1980) [in Russian].
2. J. Stock, Bull. Astron. **24**, 116 (1964).
3. Yu. N. Efremov, S. B. Novikov, and P. V. Shcheglov, Usp. Fiz. Nauk **115**, 301 (1975) [Sov. Phys. Usp. **18**, 151 (1975)].
4. S. A. Potanin, Astron. Zh. **85**, 665 (2008) [Astron. Rep. **52**, 598 (2008)].
5. M. V. Lobachev, K. M. Gruzdeva, L. E. Yakukhnova, and K. A. Chernaya, in *Methods for Increasing the Efficiency of Optical Telescopes*, Ed. by S. A. Gladyshev (Mosk. Gos. Univ., Moscow, 1987), p. 132 [in Russian].
6. B. P. Artamonov and M. I. Tertitsky, in *Methods for Increasing the Efficiency of Optical Telescopes*, Ed. by S. A. Gladyshev (Mosk. Gos. Univ., Moscow, 1987), p. 160 [in Russian].
7. B. P. Artamonov, V. V. Bruevich, O. N. Bugaenko, et al., Preprint Gos. Astron. Inst. Sternberga No. 16 (GAISh MGU, Moscow, 1990).
8. S. A. Potanin, Astron. Zh. **86**, 758 (2009) [Astron. Rep. **53**, 703 (2009)].
9. B. P. Artamonov, S. B. Novikov, and A. A. Ovchinnikov, in *Methods for Increasing the Efficiency of Optical Telescopes*, Ed. by S. A. Gladyshev (Mosk. Gos. Univ., Moscow, 1987), p. 8 [in Russian].
10. S. P. Ilyasov, A. K. Baĭzhumanov, M. Saratsin, et al., Pis'ma Astron. Zh. **25**, 156 (1999) [Astron. Lett. **25**, 122 (1999)].
11. S. A. Ehgamberdiev, A. K. Baijumanov, S. P. Ilyasov, et al., Astron. Astrophys. Suppl. Ser. **145**, 293 (2000).
12. V. G. Kornilov, S. P. Ilyasov, O. V. Vozyakova, et al., Pis'ma Astron. Zh. **35**, 606 (2009) [Astron. Lett. **35**, 547 (2009)].
13. S. B. Novikov and A. A. Ovchinnikov, in *Astroclimate and the Efficiency of Telescopes*, Ed. by V. S. Shevchenko and A. Kh. Kurmaev (Nauka, Leningrad, 1984), p. 177 [in Russian].
14. B. P. Artamonov, Proc. SPIE **2871**, 737 (1997).
15. Kh. B. Sultanov, S. P. Il'yasov, and Sh. A. Ehgamberdiev, in *Modern Problems of Astronomy in Uzbekistan*, Ed. by Sh. A. Ehgamberdiev (AI RUz AS, Tashkent, 2004), p. 21 [in Russian].
16. V. G. Vakulik, V. N. Dudinov, A. P. Zheleznyak, et al., Astron. Nachr. **318**, 73 (1997).
17. B. P. Artamonov, Yu. Yu. Badan, V. V. Bruevich, and A. S. Gusev, Astron. Zh. **76**, 438 (1999) [Astron. Rep. **43**, 377 (1999)].
18. B. P. Artamonov, Yu. Yu. Badan, and A. S. Gusev, Astron. Zh. **77**, 643 (2000) [Astron. Rep. **44**, 569 (2000)].
19. M. Sarazin and F. Roddier, Astron. Astrophys. **227**, 294 (1990).
20. T. L. Qian, C. R. Qui, X. F. Cen, et al., Acta Astron. Sinica **42**, 101 (2001).
21. B. Lim, H. Sung, M. S. Bessell, et al., J. Korean Astron. Soc. **42**, 161 (2009).

22. A. S. Gusev, Astron. Zh. **83**, 195 (2006) [Astron. Rep. **50**, 167 (2006)].
23. A. S. Gusev, Astron. Zh. **83**, 211 (2006) [Astron. Rep. **50**, 182 (2006)].
24. A. U. Landolt, Astron. J. **104**, 340 (1992).
25. G. Petrov, W. Seggewiss, A. Dieball, and B. Kovachev, Astron. Astrophys. **376**, 745 (2001).
26. M. A. Ibragimov, unpublished (2004).
27. A. P. Zheleznyak, private commun. (2004).
28. K. Zdanavichyus and D. Matsiyauskas, Byull. Vil'nyussk. Astron. Observ. **55**, 11 (1980).
29. E. Pakstiene, K. Zdanavicius, and S. Bartasiute, Baltic Astron. **10**, 651 (2001).
30. Yu. A. Tillaev, in *Modern Problems of Astronomy in Uzbekistan*, Ed. by Sh. A. Ehgamberdiev (AI Ruz AS, Tashkent, 2004), p. 34 [in Russian].
31. Yu. A. Tillaev, S. P. Il'yasov, and K. N. Grankin, Dokl. Akad. Nauk RUz **6**, 27 (2004).
32. W. J. Roberts and E. K. Grebel, Astron. Astrophys. Suppl. Ser. **109**, 313 (1995).
33. A. Jimenez, H. Gonzalez Jorge, and M. C. Rabello-Soares, Astron. Astrophys. Suppl. Ser. **129**, 413 (1998).

Translated by N. Samus'